Act1 mediates IL-17–induced EAE pathogenesis selectively in NG2$^+$ glial cells

Zizhen Kang[1,2], Chenhui Wang[2], Jarod Zepp[2], Ling Wu[2], Kevin Sun[2], Junjie Zhao[2], Unni Chandrasekharan[3], Paul E DiCorleto[3], Bruce D Trapp[4], Richard M Ransohoff[4–6] & Xiaoxia Li[2]

Interleukin 17 (IL-17) is a signature cytokine of Th17 cells. We previously reported that deletion of NF-κB activator 1 (Act1), the key transducer of IL-17 receptor signaling, from the neuroectodermal lineage in mice (neurons, oligodendrocytes and astrocytes) results in attenuated severity of experimental autoimmune encephalomyelitis (EAE). Here we examined the cellular basis of this observation. EAE disease course was unaffected by deletion of Act1 in neurons or mature oligodendrocytes, and Act1 deletion in astrocytes only modestly affected disease course. Deletion of Act1 in NG2$^+$ glia resulted in markedly reduced EAE severity. Furthermore, IL-17 induced characteristic inflammatory mediator expression in NG2$^+$ glial cells. IL-17 also exhibited strong inhibitory effects on the maturation of oligodendrocyte lineage cells *in vitro* and reduced their survival. These data identify NG2$^+$ glia as the major CNS cellular target of IL-17 in EAE. The sensitivity of oligodendrocyte lineage cells to IL-17–mediated toxicity further suggests a direct link between inflammation and neurodegeneration in multiple sclerosis.

Multiple sclerosis is a T cell–mediated inflammatory demyelinating disease of the human CNS[1]. Inflammatory demyelination is coupled with neurodegeneration in multiple sclerosis, although the precise mechanisms underlying this remain uncertain[2–4]. Many components of the myelin sheath have been injected into animals to induce EAE. Studies of the EAE model have helped to define the sequence of immunopathogenic events involved in the development of autoimmune CNS-directed inflammatory diseases[5]. During the initiation stage of EAE, in addition to T cell activation and expansion, antigen-presenting cells (APCs) produce cytokines to regulate the differentiation of effector CD4 T cells, including the classical Th1 (producing interferon-γ (IFNγ) and tumor necrosis factor α (TNFα) and Th17 (producing IL-17, IL-6 and TNFα) T cell lineages. Notably, recent studies have suggested that both Th1 and Th17 cells can independently induce EAE, possibly through different mechanisms[6,7]. Th17 cells are generated as a discrete lineage following priming in the presence of transforming growth factor β (TGFβ) and IL-6 and acquisition of encephalitogenicity following expansion in the presence of IL-23 (refs. 8–10). EAE is markedly suppressed in mice lacking IL-17 or IL-17 receptor (IL-17R), and IL-17–specific inhibition attenuates inflammation, indicating that IL-17–mediated signaling is important during the effector stage of EAE[9,11,12]. However, the precise mechanism by which IL-17 participates in EAE development and pathogenesis remains unclear.

A two-wave hypothesis has been proposed for the Th17-mediated effector stage of EAE. After priming in peripheral lymph nodes, antigen-specific Th17 cells traffic through the choroid plexus into the subarachnoid space, where they encounter antigen presented by macrophages (meningeal APCs), are restimulated and undergo clonal expansion. As a consequence of productive T cell and APC interactions, Th17 signature cytokines, including IL-17, are produced and impinge on the adjacent CNS tissue. Following activation of the parenchymal vasculature by this cytokine flux, perivascular leukocyte infiltrates accumulate, leading to the explosive inflammatory cascade associated with the onset of EAE. These re-activated Th17 cells subsequently migrate across the glia limitans basement membrane, deep into the parenchymal CNS white matter, and initiate tissue destruction, including demyelination and axonal injury.

Act1 is an essential intracellular adaptor for IL-17 signaling[13–16]. Considering the importance of Act1 in IL-17 signaling, we used Act1-deficient mice as a model system to investigate the cellular mechanism of IL-17 signaling. Previously, we found that Th17 cells efficiently infiltrate the Act1-deficient CNS, but fail to recruit additional lymphocytes, neutrophils and macrophages from the bloodstream into the CNS, indicating that IL-17–induced Act1-mediated signaling is critical for the conversion of wave 1 to wave 2 during the effector stage of EAE. Notably, targeted Act1 deficiency in neuroectoderm-derived CNS-resident cells (in *Nes-cre; Act1$^{loxP/-}$* mice), but not in endothelial cells or macrophages and microglia, significantly delayed EAE onset and reduced EAE[17]. These data indicate that IL-17 signaling directly to neuroectodermal cells is required for the pathogenic inflammation that occurs during EAE. It is important to note that, although IL-17 signaling activates the transcription factor NF-κB, inhibition of NF-κB in the neuroectodermal cells also ameliorates EAE[18,19].

NG2$^+$ glial cells, a distinct macroglial population in the adult CNS that is separate from astrocytes or oligodendrocytes[20], are closely related

[1]Shanghai Institute of Immunology, Shanghai Jiao Tong University School of Medicine, Shanghai, China. [2]Department of Immunology, Cleveland Clinic, Cleveland, Ohio, USA. [3]Department of Cellular and Molecular Medicine, Cleveland Clinic, Cleveland, Ohio, USA. [4]Department of Neuroscience, Cleveland Clinic, Cleveland, Ohio, USA. [5]Neuroinflammation Research Center, Cleveland Clinic, Cleveland, Ohio, USA. [6]Mellen Center for Mississippi Treatment and Research, Cleveland Clinic, Cleveland, Ohio, USA. Correspondence should be addressed to X.L. (lix@ccf.org).

Received 10 July; accepted 30 July; published online 1 September 2013; doi:10.1038/nn.3505

to progenitors that give rise to myelinating oligodendrocytes during development. Following varied types of CNS injury, NG2$^+$ glia proliferate and have a reactive phenotype that includes increased expression of NG2, a surface proteoglycan. Their fate *in vivo* thereafter has been a matter of some controversy, but it seems clear that they are involved in myelin repair and mainly give rise to oligodendrocytes[21]. NG2$^+$ glia have not previously been implicated in generating pathogenic inflammatory responses. We sought to define the neuroectodermal cellular target(s) of IL-17 action during EAE. After a series of negative studies, we deleted Act1 from NG2$^+$ glial cells (in *NG2* (also known as *Cspg4*)*-cre; Act1$^{loxP/-}$* mice) and virtually abrogated Th17 cell-induced EAE, recapitulating the EAE phenotype of *Nes-cre; Act1$^{loxP/-}$* mice, which lack Act1 in all neuroectodermal cells[17]. Inflammatory gene expression in response to IL-17 was nearly absent from the CNS of *NG2-cre; Act1$^{loxP/-}$* mice after Th17 cell transfers, accounting for the lack of clinical disease.

RESULTS

Ablation of Act1 from astrocytes modestly reduces EAE

Deletion of Act1 in neuroectoderm-derived cells in CNS ameliorated the severity of Th17-induced EAE[17]. Neuroectoderm-derived cells include astrocytes, neurons, NG2$^+$ glia and oligodendrocytes. Astrocytes with processes in the glia limitans and around cerebral blood vessels are positioned to transduce signals from meningeal Th17 cells to activate the blood-brain barrier endothelium and drive perivascular leukocyte infiltration (wave 2) and the consequent explosive inflammatory cascade associated with the onset of EAE. We generated astrocyte-specific Act1-deficient mice, by breeding *Act1$^{-/-}$* mice with *Gfap-cre* mice to generate *Gfap-cre; Act1$^{+/-}$* mice, and these mice were further bred onto *Act1$^{loxP/loxP}$* mice to generate control mice (*Gfap-cre; Act1$^{loxP/+}$*) and astrocyte-specific Act1-deficient mice (*Gfap-cre; Act1$^{loxP/-}$*). Western analysis revealed that Act1 expression was completely ablated in astrocytes derived from *Gfap-cre; Act1$^{loxP/-}$* mice (**Fig. 1a**).

EAE was induced in *Gfap-cre; Act1$^{loxP/-}$* mice and control mice (*Gfap-cre; Act1$^{loxP/+}$*) by active immunization with MOG_{33-55}. The astrocyte-specific *Act1*-deficient mice (*Gfap-cre; Act1$^{loxP/-}$*) showed a delay in the onset and reduced disease severity compared with the control mice (*Gfap-cre; Act1$^{loxP/+}$*). However, the EAE phenotype of the astrocyte-specific *Act1*-deficient mice was not nearly as marked as that of the CNS-restricted *Act1*-deficient mice (*Nes-cre; Act1$^{loxP/-}$*; **Fig. 1b**)[17]. When EAE was induced by adoptive transfer of MOG_{35-55}-specific wild-type Th17 cells, the *Gfap-cre; Act1$^{loxP/-}$* mice also showed a modest, but reproducible, reduction in disease severity compared with control mice (**Fig. 1c**), whereas the CNS-restricted Act1-deficient mice had delayed onset and greatly reduced EAE (**Fig. 1d**). Consistent with reduced clinical disease, mononuclear cell infiltrates were decreased in white matter of spinal cords from *Gfap-cre; Act1$^{loxP/-}$* (**Fig. 1e**,**f**). During EAE, signature IL-17–responsive inflammatory genes (cytokines, chemokines and matrix metalloproteinases) are significantly induced in CNS[2,22,23]. Induction of the IL-17–regulated inflammatory genes (including *Cxcl1*, *Cxcl2*, *Csf2*, *Il6*, *Mmp3* and *Mmp9*) in the spinal cord was substantially reduced in *Gfap-cre; Act1$^{loxP/-}$* mice, somewhat out of proportion to the clinical effect (**Fig. 1g**). Overall, our observations were similar to those reported using lentiviral shRNA to reduce Act1 expression in astrocytes[24]. Given that the EAE phenotype of astrocyte-specific Act1-deficient

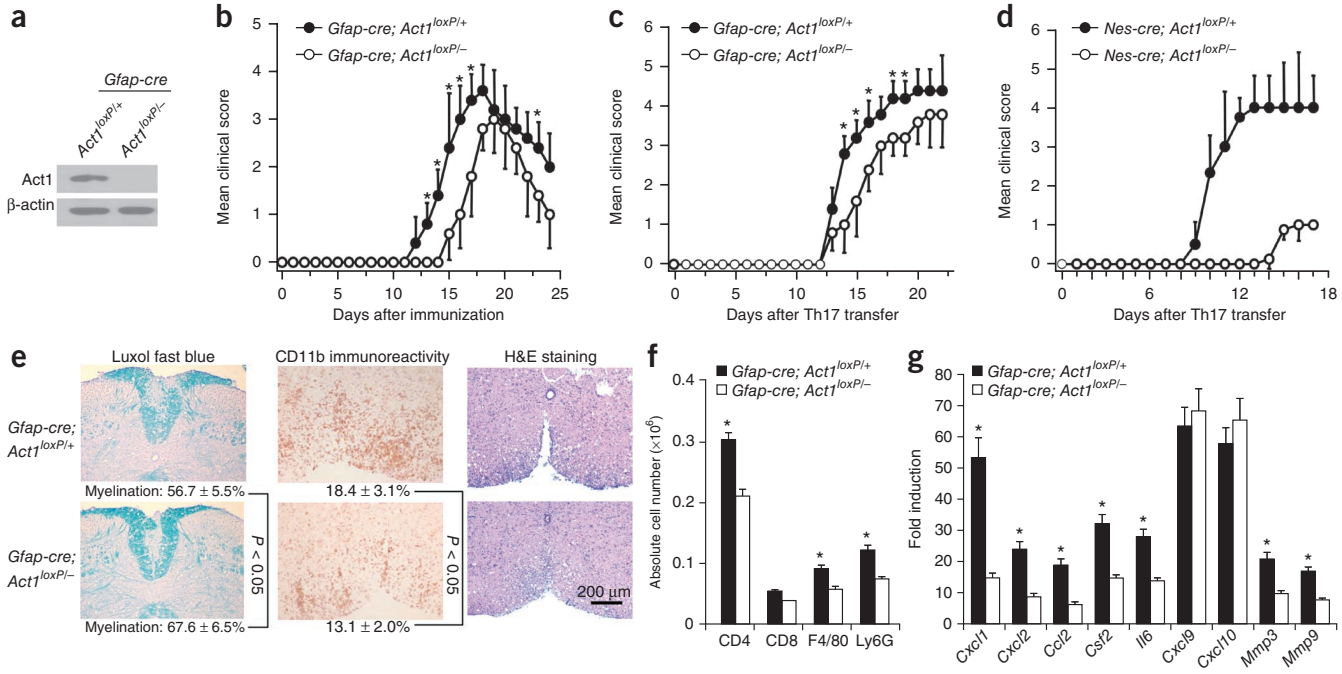

Figure 1 Ablation of Act1 in astrocytes ameliorates autoimmune encephalomyelitis. (**a**) Immunoblot analysis of Act1 expression in cultured astrocytes from neonatal *Gfap-cre; Act1$^{loxP/-}$* and control *Gfap-cre; Act1$^{loxP/+}$* mice. Full-length blots are presented in **Supplementary Figure 5**. (**b**) Mean clinical score of EAE in *Gfap-cre; Act1$^{loxP/-}$* and *Gfap-cre; Act1$^{loxP/+}$* mice induced by active immunization with MOG_{35-55}. (**c**) Mean clinical score of EAE in *Gfap-cre; Act1$^{loxP/-}$* and *Gfap-cre; Act1$^{loxP/+}$* mice induced by Th17 adoptive transfer. (**d**) Mean clinical score of EAE in *Nes-cre; Act1$^{loxP/-}$* and *Nes-cre; Act1$^{loxP/+}$* mice induced by Th17 adoptive transfer ($P < 0.05$, two-way ANOVA). (**e**) Luxol fast blue, antibody to CD11b and hematoxylin and eosin (H&E) staining of lumber spinal cords of *Gfap-cre; Act1$^{loxP/-}$* and *Gfap-cre; Act1$^{loxP/+}$* mice 20 d after Th17 adoptive transfer. Data are representative of 5 mice per group. (**f**) Absolute cell numbers of infiltrated immune cells in the brains of *Gfap-cre; Act1$^{loxP/-}$* and *Gfap-cre; Act1$^{loxP/+}$* mice 20 d after Th17 cell transfer. (**g**) Real-time PCR analysis of inflammatory gene expression in spinal cords of *Gfap-cre; Act1$^{loxP/-}$* and *Gfap-cre; Act1$^{loxP/+}$* mice 20 d after Th17 adoptive transfer. Data are representative of three independent experiments. $n = 5$ mice per group in each experiment. Error bars represent s.e.m. $^*P < 0.05$.

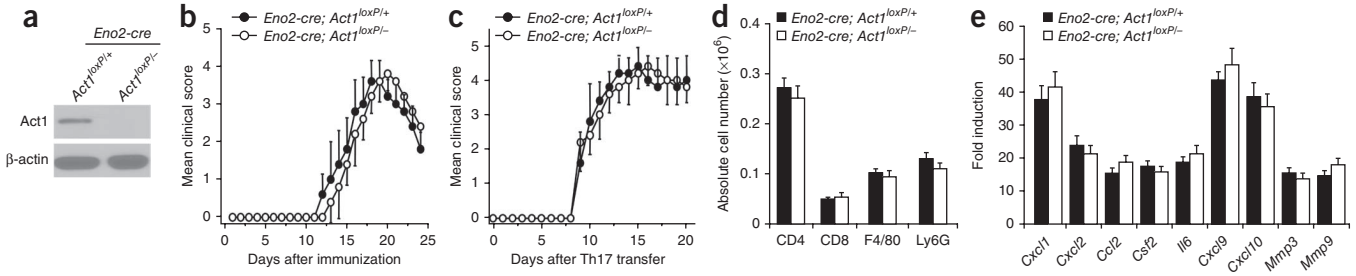

Figure 2 Neuronal Act1 is dispensable for EAE development. (**a**) Immunoblot analysis of Act1 expression in cultured neuronal cells from embryonic brains (embryonic day 14, E14) of neuron-specific Act1-deficient (*Eno2-cre; Act1*$^{loxP/-}$) and control mice (*Eno2-cre; Act1*$^{loxP/+}$). Full-length blots are presented in **Supplementary Figure 5**. (**b**) Mean clinical score of EAE in *Eno2-cre; Act1*$^{loxP/-}$ and *Eno2-cre; Act1*$^{loxP/+}$ mice induced by active immunization with MOG_{35-55}. (**c**) Mean clinical score of EAE in the *Eno2-cre; Act1*$^{loxP/-}$ and *Eno2-cre; Act1*$^{loxP/+}$ mice induced by MOG_{35-55}-specific Th17 cells. (**d**) Flow cytometric analysis of immune cell infiltration in the brains of Th17-induced *Eno2-cre; Act1*$^{loxP/-}$ and *Eno2-cre; Act1*$^{loxP/+}$ EAE mice (7 d after disease onset). (**e**) Real-time PCR analysis of inflammatory gene expression in spinal cords of *Eno2-cre; Act1*$^{loxP/-}$ and *Eno2-cre; Act1*$^{loxP/+}$ mice transferred with MOG_{35-55}-specific Th17 cells. Data are representative of three independent experiments. $n = 5$ mice per group in each experiment. Error bars represent s.e.m. $P > 0.05$ in **b**–**e**.

mice failed to reproduce that of the CNS-restricted Act1-deficient mice, we can conclude that other neuroectoderm-derived cells must also participate in Th17-mediated EAE pathogenesis.

Neuronal Act1 is dispensable for EAE development

A recent study suggested that Th17 cells directly interact with neurons, mediating neuronal dysfunction and contributing to the development of EAE[25]. To determine whether neuronal Act1 is critical for EAE pathogenesis, we generated neuronal *Act1*-deficient mice by breeding *Act1*$^{loxP/-}$ mice with *Eno2-cre* mice. Western analysis revealed that Act1 expression was abolished in neurons from the resulting *Eno2-cre; Act1*$^{loxP/-}$ mice (**Fig. 2a**). The onset and disease severity of EAE were similar in *Eno2-cre; Act1*$^{loxP/-}$ and *Eno2-cre; Act1*$^{loxP/+}$ mice after either active immunization with MOG_{35-55} or adoptive transfer of MOG_{35-55}-specific Th17 cells (**Fig. 2b**,**c**). Furthermore, inflammatory cell infiltration in the CNS of the two experimental groups was

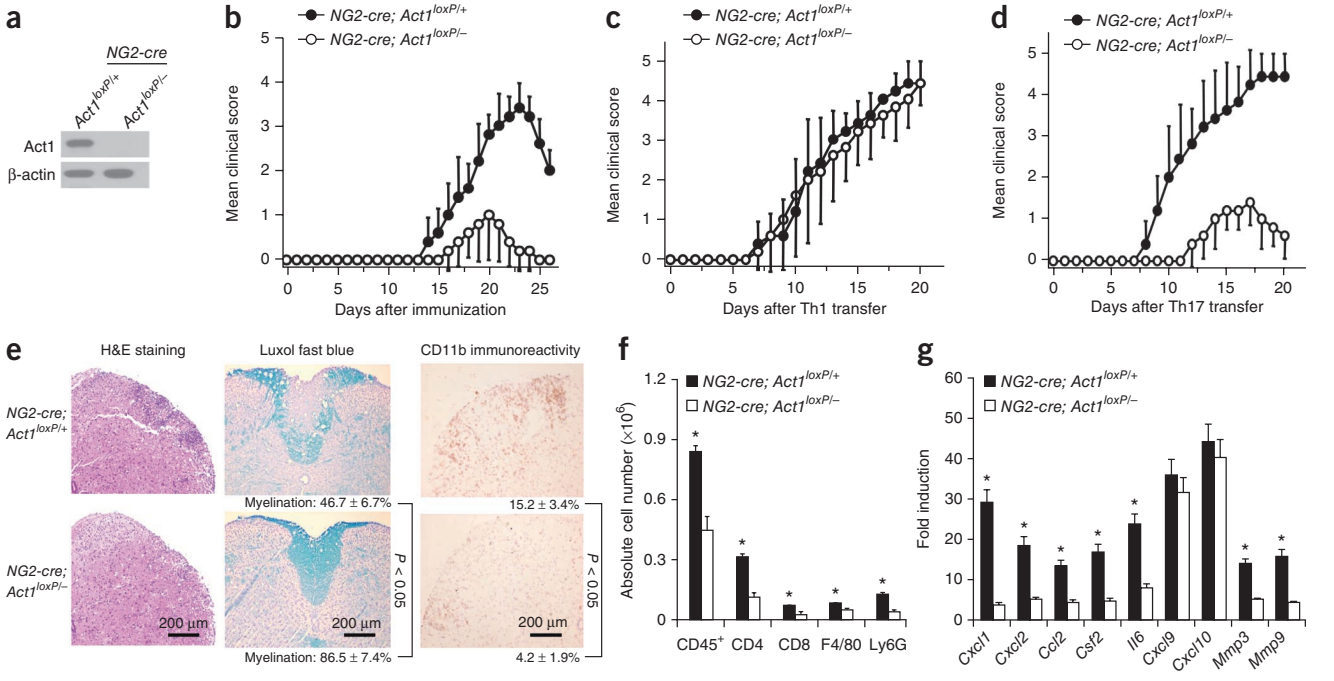

Figure 3 Ablation of Act1 in oligodendrocyte lineage ameliorates autoimmune encephalomyelitis. (**a**) Immunoblot analysis of Act1 expression in cultured NG2$^+$ OPCs from embryonic brains. Full-length blots are presented in **Supplementary Figure 5**. (**b**) Mean clinical score of EAE in *NG2-cre; Act1*$^{loxP/-}$ and *NG2-cre; Act1*$^{loxP/+}$ mice induced by active immunization with MOG_{35-55} ($P < 0.05$, two-way ANOVA). (**c**) Mean clinical score of EAE in *NG2-cre; Act1*$^{loxP/-}$ and *NG2-cre; Act1*$^{loxP/+}$ mice induced by Th1 adoptive transfer ($P > 0.05$, two-way ANOVA). (**d**) Mean clinical score of EAE in *NG2-cre; Act1*$^{loxP/-}$ and *NG2-cre; Act1*$^{loxP/+}$ mice induced by Th17 adoptive transfer ($P < 0.05$, two-way ANOVA). (**e**) Hematoxylin and eosin, luxol fast blue and CD11b immunohistochemistry of lumber spinal cords of *NG2-cre; Act1*$^{loxP/-}$ and *NG2-cre; Act1*$^{loxP/+}$ mice 20 d after Th17 adoptive transfer. Data are representative of 5 mice per group. (**f**) Absolute cell numbers of infiltrated immune cells in the brains of *NG2-cre; Act1*$^{loxP/-}$ and *NG2-cre; Act1*$^{loxP/+}$ mice (20 d after Th17 cell transfer). (**g**) Real-time PCR analysis of inflammatory gene expression in spinal cords of *NG2-cre; Act1*$^{loxP/-}$ and *NG2-cre; Act1*$^{loxP/+}$ mice that received MOG_{35-55}-specific Th17 cells. Data are representative of three independent experiments. $n = 5$ mice per group in each experiment. Error bars represent s.e.m. $^*P < 0.05$.

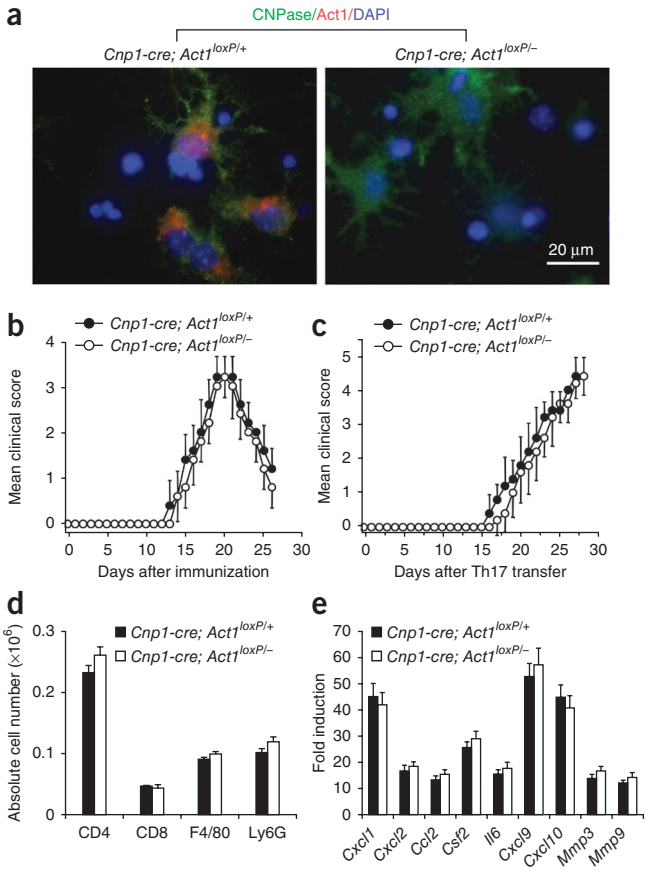

Figure 4 Act1 in mature oligodendrocytes is dispensable for the pathogenesis of EAE. (**a**) Co-staining of Act1 and CNPase in cultured oligodendrocytes from *Cnp1-cre; Act1*$^{loxP/-}$ and control mice (*Cnp1-cre; Act1*$^{loxP/+}$). (**b**) Mean clinical score of EAE in *Cnp1-cre; Act1*$^{loxP/-}$ and *Cnp1-cre; Act1*$^{loxP/+}$ mice induced by active immunization with MOG_{35-55}. (**c**) Mean clinical score of EAE in the *Cnp1-cre; Act1*$^{loxP/-}$ and *Cnp1-cre; Act1*$^{loxP/+}$ mice induced by MOG_{35-55}-specific Th17 cells. (**d**) Absolute number of immune cell infiltration in the brains of Th17-induced *Cnp1-cre; Act1*$^{loxP/-}$ and *Cnp1-cre; Act1*$^{loxP/+}$ EAE mice (20 d after Th17 transfer). (**e**) Real-time PCR analysis of inflammatory gene expression in spinal cords of *Cnp1-cre; Act1*$^{loxP/-}$ and *Cnp1-cre; Act1*$^{loxP/+}$ mice transferred with MOG_{35-55}-specific Th17 cells. Data are representative of three independent experiments. $n = 5$ mice per group in each experiment. Error bars represent s.e.m. $P > 0.05$ in **b**–**e**.

comparable after Th17 adoptive transfer (**Fig. 2d**). Neuronal Act1 deficiency had no substantial effect on inflammatory gene expression in the spinal cords of Th17-induced EAE mice (**Fig. 2e**). These data indicate that neuronal Act1 is dispensable for Th17-mediated EAE pathogenesis.

A distinct population of glial cells that express the oligodendrocyte progenitor cell (OPC) markers NG2 and PDGFRα persists throughout the adult CNS[20,26]. These glia (termed NG2 glia or polydendrocytes) can give rise to myelinating oligodendrocytes *in vitro* or *in vivo*. They show brisk morphological responses to injury of the CNS. Their physiological roles in the adult CNS have been extensively studied, but remain incompletely understood[21,27–29]. We used *Ng2-cre* mice[20,30] to mediate specific deletion of Act1 in oligodendrocyte-lineage cells, including developmental OPCs, mature oligodendrocytes and NG2$^+$ glia of the adult CNS. *Act1*$^{-/-}$ mice were first bred with *NG2-cre* mice to generate *NG2-cre; Act1*$^{+/-}$ mice. These mice were further bred with *Act1*$^{loxP/loxP}$ mice to generate *NG2-cre; Act1*$^{loxP/+}$ and *NG2-cre; Act1*$^{loxP/-}$ mice. Immunoblot revealed that Act1 expression was completely ablated in NG2$^+$ cells derived from *NG2-cre; Act1*$^{loxP/-}$ mice (**Fig. 3a**).

We induced EAE in *NG2-cre; Act1*$^{loxP/-}$ mice and control mice (*NG2-cre; Act1*$^{loxP/+}$) by active immunization with MOG_{33-55}. Notably, Act1 deficiency in NG2$^+$ glia delayed the onset of EAE and greatly reduced the disease severity (**Fig. 3b**), similar to *NG2-cre; Act1*$^{loxP/-}$ mice. It is important to note that the MOG-induced T cell priming was comparable in *NG2-cre; Act1*$^{loxP/-}$ and *NG2-cre; Act1*$^{loxP/+}$ mice (**Supplementary Fig. 1b**). Furthermore, Th17 cells from MOG-immunized *NG2-cre; Act1*$^{loxP/-}$ and *NG2-cre; Act1*$^{loxP/+}$ mice induced similar EAE in wild-type recipient mice (**Supplementary Fig. 1c–e**). These data suggest that the resistance of *NG2-cre; Act1*$^{loxP/-}$ mice to EAE induced by active immunization with MOG_{33-55} (**Fig. 3b**) probably occurred at the effector stage of EAE. To confirm this interpretation, we used both *NG2-cre; Act1*$^{loxP/+}$ and *NG2-cre; Act1*$^{loxP/-}$ mice as recipients of activated wild-type MOG_{35-55}-specific Th1 or Th17 cells. Although the Th1 cells induced a similar EAE phenotype in both groups of mice, the onset and severity of Th17 cell–induced EAE were greatly reduced in *NG2-cre; Act1*$^{loxP/-}$ compared with control mice (**Fig. 3c**,**d**). The *NG2-cre; Act1*$^{loxP/-}$ mice had fewer inflammatory cells in the CNS, including CD4$^+$ and CD8$^+$ T cells, macrophages, and neutrophils, than control mice at the peak of disease after Th17 cell transfer (**Fig. 3e**,**f** and **Supplementary Fig. 1a**). Th17-associated, but not Th1-related, inflammatory gene expression levels in the spinal cords of *NG2-cre; Act1*$^{loxP/-}$ mice were markedly reduced compared with control mice (**Fig. 3g**). Collectively, these data indicate that, among the neuroectoderm-derived cells, NG2$^+$ glia are important for the occurrence of Th17-mediated EAE.

What is the effect of Act1 deficiency on NG2$^+$ cells and mature oligodendrocytes during EAE? The numbers of NG2$^+$ cells and mature oligodendrocytes were comparable in the spinal cords of naive *NG2-cre; Act1*$^{loxP/+}$ and *NG2-cre; Act1*$^{loxP/-}$ mice (**Supplementary Fig. 2a**,**b**). Mature GST-π$^+$ oligodendrocytes were substantially reduced in the spinal cords of *NG2-cre; Act1*$^{loxP/+}$ mice after EAE induction (**Supplementary Fig. 2a**). In contrast, NG2$^+$ cells were markedly increased in *NG2-cre; Act1*$^{loxP/+}$ mice, whereas NG2$^+$ glial cell numbers were unchanged in *NG2-cre; Act1*$^{loxP/-}$ mice (**Supplementary Fig. 2b**). Consistently, BrdU incorporation in NG2$^+$ cells was much greater in the spinal cords of *NG2-cre; Act1*$^{loxP/+}$ mice than in *NG2-cre; Act1*$^{loxP/-}$ mice (**Supplementary Fig. 2c**). These results suggest that NG2$^+$ cells were activated during EAE (as evident by increased BrdU incorporation and NG2$^+$ cell numbers), indicating that these cells might participate in the inflammatory cascade that underlies EAE pathogenesis.

However, it is also plausible that the ability of NG2$^+$ glia to participate at later time points in myelin repair might be perturbed by IL-17–induced Act1-mediated signaling, as shown by a decrease in the number of mature oligodendrocytes in *NG2-cre; Act1*$^{loxP/+}$ mice after Th17 EAE induction (**Supplementary Fig. 2a**). Notably, following Th1 induction of EAE, both *NG2-cre; Act1*$^{loxP/-}$ mice and control mice had similar levels of demyelination, as seen by myelin basic protein (MBP) staining (**Supplementary Fig. 2d**).

NG2$^+$ glial cells, a distinct macroglial population in the adult CNS, separate from astrocytes or oligodendrocytes[20], are closely related to progenitors that give rise to myelinating oligodendrocytes during development or in response to CNS injury. Our results suggest that IL-17 signaling in NG2$^+$ cells might incorporate these glia into the inflammatory pathogenesis of EAE. In particular, the reactive phenotype of increased proliferation and cell number supports this interpretation. However, it is possible that the EAE-resistant phenotype of

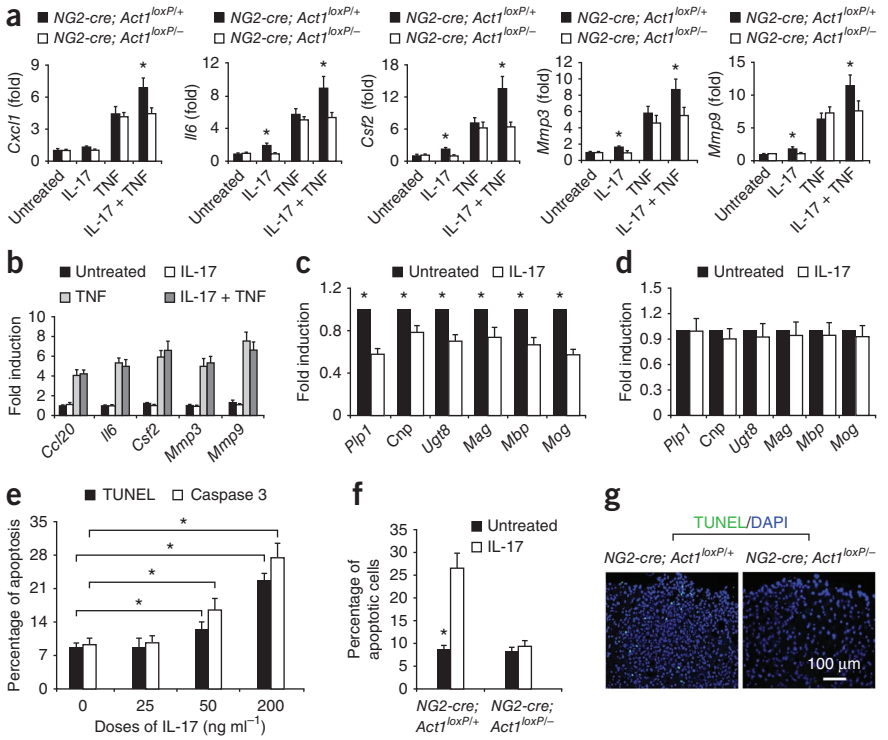

Figure 5 Cytotoxic and inflammatory effects of IL-17–induced Act1-mediated signaling on oligodendroglia. After 4 d in culture with a cytokine cocktail of FGF and PDGF, >98% of the neural stem cells became Olig2$^+$ CNPase$^-$ cells, suggesting that they were OPCs. Cytokines were then withdrawn to drive the maturation of OPC for 2 d. Immunohistochemical staining revealed that >95% cells were CNPase$^+$ GFAP$^-$ β-tubulin III$^-$, suggesting that they were mature oligodendrocytes. (**a**) OPCs from *NG2-cre; Act1$^{loxP/+}$* and *NG2-cre; Act1$^{loxP/-}$* mice were treated with IL-17 (25 ng ml^{-1}), TNF (10 ng ml^{-1}) or IL-17 and TNF for 6 h. Indicated gene expression was quantified by real-time PCR. (**b**) Mature oligodendrocytes from wild-type mice were treated with IL-17 (25 ng ml^{-1}), TNF (10 ng ml^{-1}) or IL-17 and TNF for 6 h. Indicated gene expression was quantified by real-time PCR. (**c**,**d**) OPCs from *NG2-cre; Act1$^{loxP/+}$* mice (**c**) and *NG2-cre; Act1$^{loxP/-}$* mice (**d**) were cultured for another 2 d without FGF and PDGF, but with or without addition of IL-17 (25 ng ml^{-1}). Myelin-related gene expression was quantified by real-time PCR. (**e**) TUNEL and cleaved caspase 3 assays for of wild-type OPCs after 4 d in culture with or without IL-17. 1,500 cells were scored from 15 power fields from 5 slices from 5 mice. (**f**) Data shown are the apoptotic percentages of OPCs from *NG2-cre; Act1$^{loxP/+}$* mice and *NG2-cre; Act1$^{loxP/-}$* mice after 4 d in culture with or without IL-17 (200 ng ml^{-1}). (**g**) TUNEL assay of apoptotic cells in the lumber spinal cord of *NG2-cre; Act1$^{loxP/+}$* and *NG2-cre; Act1$^{loxP/-}$* mice 20 d after Th17 adoptive transfer. Apoptotic cells were counted from five sections of each mouse and then got the mean value per section. Data are representative of three independent experiments. $n = 5$ mice per group in each experiment. Error bars represent s.e.m. $^*P < 0.05$.

NG2-cre; Act1$^{loxP/-}$ mice could be attributed, in whole or in part, to deletion of Act1 from NG2$^+$ vessel-associated pericytes; thus, we used *Olig2-cre* mice to mediate the deletion of Act1 in the oligodendrocyte lineage[31–33] (**Supplementary Fig. 3a**). Act1 deficiency in Olig2$^+$ cells delayed the onset of EAE and greatly reduced the disease severity following active immunization with $MOG_{35–55}$ (**Supplementary Fig. 3b**). Furthermore, the onset and severity of Th17 cell–induced EAE were greatly reduced in *Olig2-cre; Act1$^{loxP/-}$* mice compared with that in control mice, whereas the Th1 cells induced a similar EAE phenotype in both groups of mice (**Supplementary Fig. 3c**,**d**). The *Olig2-cre; Act1$^{loxP/-}$* mice had fewer inflammatory cells in CNS than control mice at the peak of disease after Th17 cell transfer (**Supplementary Fig. 3e**). Th17-associated, but not Th1-related, inflammatory gene expression levels in the spinal cords of *Olig2-cre; Act1$^{loxP/-}$* mice were marked reduced compared with control mice (**Supplementary Fig. 3f**). The EAE phenotypes of *Nes-cre; Act1$^{loxP/-}$* mice, *NG2-cre; Act1$^{loxP/-}$* mice and *Olig2-cre; Act1$^{loxP/-}$* mice were virtually identical, supporting the hypothesis that the neuroepithelial cell whose response to IL-17 was crucial for EAE pathogenesis was the NG2$^+$glial cell.

Given that the *NG2-cre* transgene mediates deletion of *loxP*-flanked sequences in oligodendrocyte-lineage cells during development, as well as in the NG2$^+$ glia in the adult, we asked whether mature oligodendrocyte–derived Act1 is important for EAE development. *Cnp1* (also known as CNPase) promoter activity is low in OPCs, but gradually increases during oligodendrocyte differentiation and remains high in mature oligodendrocytes[26,32,34,35]. Thus, *Cnp1-cre* transgenic mice have been invaluable for deleting target genes in mature oligodendrocytes[35–37]. Immunohistochemical staining revealed that Act1 expression was completely ablated in CNP1$^+$ cells derived from *Cnp1-cre; Act1$^{loxP/-}$* mice (**Fig. 4a**). Both immunization with $MOG_{35–55}$ and adoptive transfer of activated $MOG_{35–55}$–specific Th17 cells resulted in similar onset and disease severity of EAE in the *Cnp1-cre; Act1$^{loxP/-}$* mice compared with control mice (**Fig. 4b**,**c**). Cell infiltration was also analyzed by flow cytometry after Th17 adoptive transfer. There were comparable levels of cell infiltration in the CNS tissues derived from these two groups of mice (**Fig. 4d**). Furthermore, real-time PCR revealed similar levels of induction of inflammatory genes in the spinal cords of *Cnp1-cre; Act1$^{loxP/-}$* mice and *Cnp1-cre; Act1$^{loxP/+}$* controls (**Fig. 4e**). Together, these data indicate that mature oligodendrocyte–derived Act1 is dispensable for the pathogenesis of EAE.

Inflammatory and cytotoxic effects of IL-17 on NG2$^+$ glia

Deletion of Act1 from mature oligodendrocytes had no effect on Th17-mediated EAE, whereas Act1 deficiency in NG2$^+$ glia decisively altered EAE pathogenesis. What responses of NG2$^+$ glia to IL-17 might mediate these effects on EAE severity? To answer this question, we cultured embryonic neurospheres to generate OPCs and mature oligodendrocytes. After 4 d of culture in cytokine cocktail of fibroblast grown factor (FGF) and platelet-derived growth factor (PDGF), the neural stem cells had differentiated into OPCs (>98% Olig2$^+$ CNPase$^-$). The OPCs were then induced to mature into oligodendrocytes by withdrawing growth factors. At the end of 2 d of maturation, >95% cells were mature oligodendrocytes (CNPase$^+$ GFAP$^-$ β-tubulin-III$^-$; **Supplementary Fig. 4a**,**b**). IL-17–induced robust inflammatory responses in OPCs, whereas we detected little inflammatory response in mature oligodendrocytes (**Fig. 5a**,**b**). This inflammatory response in OPCs was Act1 dependent. These results are consistent with our hypothesis that NG2$^+$ glia constitute an essential component of the CNS inflammatory response in Th17-induced EAE.

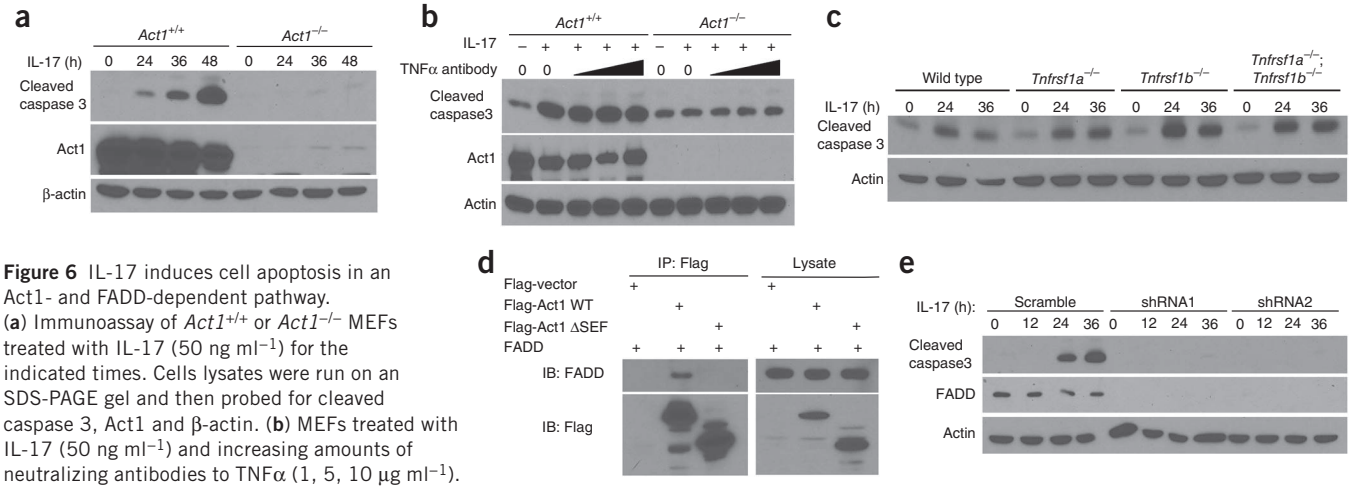

Figure 6 IL-17 induces cell apoptosis in an Act1- and FADD-dependent pathway. (**a**) Immunoassay of *Act1*$^{+/+}$ or *Act1*$^{-/-}$ MEFs treated with IL-17 (50 ng ml^{-1}) for the indicated times. Cells lysates were run on an SDS-PAGE gel and then probed for cleaved caspase 3, Act1 and β-actin. (**b**) MEFs treated with IL-17 (50 ng ml^{-1}) and increasing amounts of neutralizing antibodies to TNFα (1, 5, 10 μg ml^{-1}). (**c**) Immunoblot analysis of wild-type, *Tnfrsf1a*$^{-/-}$, *Tnfrsf1b*$^{-/-}$, and *Tnfrsf1a*$^{-/-}$*; Tnfrsf1b*$^{-/-}$ kidney epithelial cells treated with IL-17 (200 ng ml^{-1}) for the indicated times. (**d**) HEK293 cells were transfected with Flag-tagged Act1, FADD and vector control. Lysates were immunoprecipitated with antibody to Flag. (**e**) Immunoassay of OPCs transduced with lentiviral scrambled shRNA or FADD-targeting shRNA1 or shRNA2. Cells were untreated or were treated with IL-17 (200 ng ml^{-1}). Cell lysates were blotted as indicated. Data are representative of at least three independent experiments. Full-length blots are presented in **Supplementary Figure 6**.

We also asked whether IL-17 action toward OPCs might affect myelin repair following demyelination. The addition of IL-17 to OPCs from *NG2-cre; Act1*$^{loxP/+}$ mice (**Fig. 5c**), but not *NG2-cre; Act1*$^{loxP/-}$ mice (**Fig. 5d**), substantially reduced the expression of myelin proteins and other markers associated with myelinating oligodendrocytes, suggesting that commitment to an inflammatory program of gene expression might impair the ability of these cells to engage in the process of remyelination. Notably, IL-17 also induced dose-dependent cell apoptosis during the differentiation of OPCs to oligodendrocytes (**Fig. 5e** and **Supplementary Fig. 4c**), and this effect was abolished in *NG2-cre; Act1*$^{loxP/-}$ OPCs (**Fig. 5f**). TUNEL assay revealed increased cell death in the parenchyma of spinal cords from *NG2-cre; Act1*$^{loxP/+}$ mice as compared with *NG2-cre; Act1*$^{loxP/-}$ mice (43.0 ± 8.3 versus 5.0 ± 3.3 apoptotic cells per section) after Th17 adoptive transfer (**Fig. 5g**). Taken together, these data indicate that IL-17 exerts neurotoxic effects on OPCs *in vitro* and, by extension, could mediate such effects *in vivo*. As inflammation and neurodegeneration are the cardinal pathogenic processes of multiple sclerosis, these results may have important implications for the human disease. We also examined the effect of IL-17 treatment on cultured astrocytes and neurons. Consistent with our previous findings[17], although IL-17 induced an inflammatory response in astrocytes from both *NG2-cre; Act1*$^{loxP/+}$ and *NG2-cre; Act1*$^{loxP/-}$ mice, neurons from either group of mice were barely responsive to IL-17 (data not shown). It is intriguing to note that IL-17 also induced apoptosis in astrocytes from *NG2-cre; Act1*$^{loxP/+}$ and *NG2-cre; Act1*$^{loxP/-}$ mice, indicating that IL-17–induced apoptosis is not restricted to OPCs (data not shown). However, IL-17 stimulation failed to induce apoptosis in neurons (data not shown). Thus, these *ex vivo* results are consistent with our *in vivo* EAE phenotypes: although ablation of Act1 from astrocytes modestly reduced autoimmune encephalomyelitis, neuronal Act1 was dispensable for EAE development.

Although much effort has been devoted to the study of IL-17–induced inflammatory response, it is equally important to understand how IL-17 mediates cell apoptosis. Notably, we found that IL-17 induced caspase 3 cleavage in wild-type mouse embryonic fibroblasts (MEFs), but not in Act1-deficient MEFs (**Fig. 6a**), confirming that IL-17–induced apoptosis is not restricted to OPCs. Although a recent study suggested that IL-17 can synergize with TNFα to induce apoptosis[38], we found that TNFα neutralization did not affect IL-17–induced apoptosis in MEFs (**Fig. 6b**). Furthermore, IL-17 induced apoptosis in *Tnfrsf1a* and *Tnfrsf1b* single and double knockout kidney epithelial cells (**Fig. 6c**). These results indicate that IL-17 induces apoptosis independently of TNF-α, but do not answer how Act1 signaling intersects with apoptotic pathways. We found that Act1 interacted with FADD, a death domain–containing adaptor in the cell death pathway (**Fig. 6d**). A recent study showed that IL-25 (IL-17E) receptor interacts with the death domain of FADD though the SEFIR domain[39]. Given that Act1 also contains a SEFIR domain and interacts with FADD, we hypothesized that IL-17R might recruit FADD through Act1's SEFIR domain. We found that the SEFIR domain of Act1 was indeed required for its interaction with FADD (**Fig. 6d**), and IL-17 failed to induce apoptosis in OPCs from which FADD was depleted by shRNA-mediated knockdown (**Fig. 6e**). These data implicate the IL-17R–Act1–FADD axis as a new pathway for cell apoptosis.

DISCUSSION

The mechanisms by which IL-17 contributes to EAE pathogenesis have remained obscure. Previously, we found that targeted Act1 deficiency in neuroectoderm-derived CNS resident cells results in markedly reduced EAE severity[17], suggesting that IL-17 operates in the CNS to cause disease manifestation. Here, we used genetic models to address the cellular basis of this observation. We abrogated IL-17 signaling in astrocytes, oligodendroglial-lineage cells or neurons to directly examine how Th17-mediated demyelination and neurodegeneration proceed during EAE. Several notable observations emerged during these experiments. First, our results provide definitive genetic evidence that IL-17 signaling to Act1 in astrocytes has only a modest role in the severity of EAE. Given that GFAP is also expressed by a small fraction of neural stem cells, it is possible that GFAP$^+$ stem cell–derived NG2$^+$ glia might partially account for the phenotype observed in *Gfap-cre; Act1*$^{loxP/-}$ mice. However, western analysis revealed that the sorted NG2$^+$ glial cells from both *Gfap-cre; Act1*$^{loxP/-}$ and *Gfap-cre; Act1*$^{loxP/+}$ mice had similar levels of Act1 (data not shown). Thus, the reduced EAE phenotype observed in *Gfap-cre; Act1*$^{loxP/-}$ mice is probably a result of the reduced inflammatory response of the astrocytes in these mice. Notably, the deletion of Act1 from NG2$^+$ glial cells markedly reduced the severity of Th17 cell–induced EAE and recapitulated the

EAE phenotype of mice that lacked Act1 in all neuroectodermal cells. Act1 deficiency in mature oligodendrocytes or neurons had no effect on EAE severity. The EAE-resistant phenotype of *NG2-cre; Act1$^{loxP/-}$* mice was attributable to IL-17 signaling to NG2$^+$ glia, rather than pericytes, as we observed an identical phenotype in *Olig2-cre; Act1$^{loxP/-}$* mice. NG2$^+$ glial cell deficiency for Act1 coordinately reduced clinical severity and inflammatory infiltrates. Furthermore, inflammatory gene expression analysis of tissue from *NG2-cre; Act1$^{loxP/-}$* mice with EAE revealed a virtual absence of IL-17–induced genes, such as *Cxcl1* and *Cxcl2*, but we found no effect on the IFN-γ–induced chemokines CXCL9 and CXCL10. The same gene expression pattern was observed *in vitro* using cells derived from these mice. These results identify a previously unknown CNS-resident cellular target for IL-17–mediated EAE pathogenesis. It has been remarked on several occasions that NG2$^+$ glia show morphological transformation in response to inflammation[40,41]. To date, the microglia and astrocytes have been considered to be the major reactive glial elements of the CNS. Our results represent, to the best of our knowledge, the first insight into specific pathogenic effects of NG2$^+$ glial cell neuroinflammation.

Consistent with the *in vivo* EAE phenotype, IL-17 induced inflammatory gene expression in OPCs derived *in vitro* from neurosphere cells. Although NG2$^+$ cells are also referred to as OPCs, about 85% of the cultured OPCs are NG2$^+$ cells in our culture system. Together with our *in vivo* findings, the observed IL-17–induced inflammatory response in OPCs strongly supports the interpretation that NG2$^+$ cells *in vivo* are involved in IL-17–dependent inflammatory response during EAE. In support of this, we found that *NG2-cre*–mediated Act1 deletion substantially reduced Th17-induced inflammatory gene expression in the spinal cord during EAE. Eliminating Act1 signaling from GFAP$^+$ astrocytes also moderately reduced the severity of EAE and lessened expression of Th17-associated, but not Th1-associated, chemokines. Comparable effects were recently obtained by intrathecal lentiviral delivery of Act1 shRNA using an expression cassette that targeted astrocytes[24].

Multiple sclerosis (and the EAE model) results in both inflammatory and neurodegenerative damage to the CNS tissue. The relationship between inflammation and neurodegeneration has been controversial and difficult to resolve. Recent important reports have suggested that removal of myelin renders axons metabolically nonviable, placing intense emphasis on understanding mechanisms by which myelin repair either occurs or fails[42,43]. We also found that IL-17 affected survival and maturation of OPCs derived *in vitro* from neurosphere cells. Following varied types of CNS injury, NG2$^+$ glia proliferate and are involved in myelin repair and mainly give rise to oligodendrocytes[21]. We found that, although NG2$^+$ cells were indeed activated during EAE (as evident by increased BrdU incorporation and NG2$^+$ cell numbers), mature oligodendrocytes were substantially reduced in the spinal cords of *NG2-cre; Act1$^{loxP/+}$* mice compared with those in *NG2-cre; Act1$^{loxP/-}$* mice. These results suggest that the NG2$^+$ glia may indeed function as precursors and progenitors (OPCs) *in vivo* and their ability to participate in the repair of demyelination might be perturbed by IL-17–induced Act1-mediated signaling. Taken together, these *ex vivo* and *in vivo* observations suggest that IL-17 mediates neurotoxic effects toward NG2 glia in EAE, in addition to eliciting pronounced pathogenic inflammatory responses from these cells. Impaired remyelination has marked consequence for the progressive loss of demyelinated axons and functional deficits. The remyelination process involves the proliferation and maturation of NG2 cells, which are widely distributed through adult CNS and remain committed to the oligodendrocyte lineage[44,45].

The importance of cell apoptosis in the pathogenesis of EAE has been extensively studied. Both extrinsic and intrinsic pathways of apoptosis affect EAE development[46–49]. The death of oligodendrocytes not only causes direct demyelination, but also releases danger signals that further induce sterile inflammation. Moreover, the debris from the dead cells provides abundant self-antigens that continuously reactivate infiltrated T cells. Thus, inflammation and cell death constitute a positive feedback loop in CNS autoimmune inflammation[50]. In conclusion, our *in vitro* data suggest that IL-17 has neurotoxic effects and is involved in the pathogenesis of EAE, which is supported by our observation of increased numbers of apoptotic cells in tissue from EAE mice with intact Act1 signaling in NG2$^+$ glia. Taken together, our data suggest that the immune and neurotoxic effects of IL-17 toward glial cells (predominantly NG2$^+$ glia) provide a crucial link joining the inflammatory and neurodegenerative aspects of multiple sclerosis.

METHODS

Methods and any associated references are available in the online version of the paper.

Note: Any Supplementary Information and Source Data files are available in the online version of the paper.

ACKNOWLEDGMENTS

We gratefully acknowledge W.B. Stallcup (Burnham Institute for Medical Research) for providing antibodies to NG2 and K.-A. Nave for providing *Cnp1-cre* transgenic mice (Max Planck Institute of Experimental Medicine). We also thank the Dana-Farber Cancer Institute for providing the *Olig2-cre* transgenic mice. This investigation was supported by grants from the US National Institutes of Health (R01NS071996 and P01HL103453).

AUTHOR CONTRIBUTIONS

Z.K. designed and performed most of the experiments, interpreted the data, and wrote part of the manuscript. C.W. carried out most of the western blotting. J. Zepp did some western blotting and manuscript editing. L.W. performed some immunohistochemical staining. K.S. aided in western blotting, immunohistochemical staining and real-time PCR. J. Zhao performed statistical analysis. U.C. executed mouse breeding and cell culture. P.E.D. helped with experimental design. B.D.T. interpreted data. R.M.R. contributed to experimental design and manuscript writing. X.L. was integral for experimental design, manuscript writing, data interpretation and project coordination.

COMPETING FINANCIAL INTERESTS

The authors declare no competing financial interests.

1. Sawcer, S. *et al.* Genetic risk and a primary role for cell-mediated immune mechanisms in multiple sclerosis. *Nature* **476**, 214–219 (2011).
2. Becher, B., Bechmann, I. & Greter, M. Antigen presentation in autoimmunity and CNS inflammation: how T lymphocytes recognize the brain. *J. Mol. Med. (Berl)* **84**, 532–543 (2006).
3. Sospedra, M. & Martin, R. Immunology of multiple sclerosis. *Annu. Rev. Immunol.* **23**, 683–747 (2005).
4. Steinman, L. Multiple sclerosis: a two-stage disease. *Nat. Immunol.* **2**, 762–764 (2001).
5. Ransohoff, R.M. Animal models of multiple sclerosis: the good, the bad and the bottom line. *Nat. Neurosci.* **15**, 1074–1077 (2012).
6. Stromnes, I.M., Cerretti, L.M., Liggitt, D., Harris, R.A. & Goverman, J.M. Differential regulation of central nervous system autoimmunity by T(H)1 and T(H)17 cells. *Nat. Med.* **14**, 337–342 (2008).
7. Kroenke, M.A., Carlson, T.J., Andjelkovic, A.V. & Segal, B.M. IL-12– and IL-23–modulated T cells induce distinct types of EAE based on histology, CNS chemokine profile and response to cytokine inhibition. *J. Exp. Med.* **205**, 1535–1541 (2008).
8. Cua, D.J. *et al.* Interleukin-23 rather than interleukin-12 is the critical cytokine for autoimmune inflammation of the brain. *Nature* **421**, 744–748 (2003).
9. Veldhoen, M., Hocking, R.J., Atkins, C.J., Locksley, R.M. & Stockinger, B. TGFbeta in the context of an inflammatory cytokine milieu supports *de novo* differentiation of IL-17–producing T cells. *Immunity* **24**, 179–189 (2006).

10. Mangan, P.R. *et al.* Transforming growth factor–beta induces development of the T(H)17 lineage. *Nature* **441**, 231–234 (2006).
11. Komiyama, Y. *et al.* IL-17 plays an important role in the development of experimental autoimmune encephalomyelitis. *J. Immunol.* **177**, 566–573 (2006).
12. Hu, Y. *et al.* IL-17RC is required for IL-17A– and IL-17F–dependent signaling and the pathogenesis of experimental autoimmune encephalomyelitis. *J. Immunol.* **184**, 4307–4316 (2010).
13. Li, X. *et al.* Act1, an NF-kappa B–activating protein. *Proc. Natl. Acad. Sci. USA* **97**, 10489–10493 (2000).
14. Leonardi, A., Chariot, A., Claudio, E., Cunningham, K. & Siebenlist, U. CIKS, a connection to Ikappa B kinase and stress-activated protein kinase. *Proc. Natl. Acad. Sci. USA* **97**, 10494–10499 (2000).
15. Qian, Y., Zhao, Z., Jiang, Z. & Li, X. Role of NF kappa B activator Act1 in CD40-mediated signaling in epithelial cells. *Proc. Natl. Acad. Sci. USA* **99**, 9386–9391 (2002).
16. Qian, Y. *et al.* The adaptor Act1 is required for interleukin 17–dependent signaling associated with autoimmune and inflammatory disease. *Nat. Immunol.* **8**, 247–256 (2007).
17. Kang, Z. *et al.* Astrocyte-restricted ablation of interleukin-17–induced Act1-mediated signaling ameliorates autoimmune encephalomyelitis. *Immunity* **32**, 414–425 (2010).
18. Raasch, J. *et al.* IkappaB kinase 2 determines oligodendrocyte loss by non-cell-autonomous activation of NF-kappaB in the central nervous system. *Brain* **134**, 1184–1198 (2011).
19. van Loo, G. *et al.* Inhibition of transcription factor NF-κB in the central nervous system ameliorates autoimmune encephalomyelitis in mice. *Nat. Immunol.* **7**, 954–961 (2006).
20. Nishiyama, A., Komitova, M., Suzuki, R. & Zhu, X. Polydendrocytes (NG2 cells): multifunctional cells with lineage plasticity. *Nat. Rev. Neurosci.* **10**, 9–22 (2009).
21. Richardson, W.D., Young, K.M., Tripathi, R.B. & McKenzie, I. NG2-glia as multipotent neural stem cells: fact or fantasy? *Neuron* **70**, 661–673 (2011).
22. Gold, R., Linington, C. & Lassmann, H. Understanding pathogenesis and therapy of multiple sclerosis via animal models: 70 years of merits and culprits in experimental autoimmune encephalomyelitis research. *Brain* **129**, 1953–1971 (2006).
23. Weaver, A. *et al.* An elevated matrix metalloproteinase (MMP) in an animal model of multiple sclerosis is protective by affecting Th1/Th2 polarization. *FASEB J.* **19**, 1668–1670 (2005).
24. Yan, Y. *et al.* CNS-specific therapy for ongoing EAE by silencing IL-17 pathway in astrocytes. *Mol. Ther.* **20**, 1338–1348 (2012).
25. Siffrin, V. *et al. In vivo* imaging of partially reversible Th17 cell–induced neuronal dysfunction in the course of encephalomyelitis. *Immunity* **33**, 424–436 (2010).
26. Baumann, N. & Pham-Dinh, D. Biology of oligodendrocyte and myelin in the mammalian central nervous system. *Physiol. Rev.* **81**, 871–927 (2001).
27. Fancy, S.P., Chan, J.R., Baranzini, S.E., Franklin, R.J. & Rowitch, D.H. Myelin regeneration: a recapitulation of development? *Annu. Rev. Neurosci.* **34**, 21–43 (2011).
28. Trotter, J., Karram, K. & Nishiyama, A. NG2 cells: Properties, progeny and origin. *Brain Res. Rev.* **63**, 72–82 (2010).
29. Menn, B. *et al.* Origin of oligodendrocytes in the subventricular zone of the adult brain. *J. Neurosci.* **26**, 7907–7918 (2006).
30. Zhu, X., Bergles, D.E. & Nishiyama, A. NG2 cells generate both oligodendrocytes and gray matter astrocytes. *Development* **135**, 145–157 (2008).
31. Emery, B. *et al.* Myelin gene regulatory factor is a critical transcriptional regulator required for CNS myelination. *Cell* **138**, 172–185 (2009).
32. Zhou, Q., Wang, S. & Anderson, D.J. Identification of a novel family of oligodendrocyte lineage–specific basic helix-loop-helix transcription factors. *Neuron* **25**, 331–343 (2000).
33. Schüller, U. *et al.* Acquisition of granule neuron precursor identity is a critical determinant of progenitor cell competence to form Shh-induced medulloblastoma. *Cancer Cell* **14**, 123–134 (2008).
34. Yu, W.P., Collarini, E.J., Pringle, N.P. & Richardson, W.D. Embryonic expression of myelin genes: evidence for a focal source of oligodendrocyte precursors in the ventricular zone of the neural tube. *Neuron* **12**, 1353–1362 (1994).
35. Lappe-Siefke, C. *et al.* Disruption of Cnp1 uncouples oligodendroglial functions in axonal support and myelination. *Nat. Genet.* **33**, 366–374 (2003).
36. Dugas, J.C. *et al.* Dicer1 and miR-219 are required for normal oligodendrocyte differentiation and myelination. *Neuron* **65**, 597–611 (2010).
37. Kaga, Y. *et al.* Mice with conditional inactivation of fibroblast growth factor receptor-2 signaling in oligodendrocytes have normal myelin, but display dramatic hyperactivity when combined with Cnp1 inactivation. *J. Neurosci.* **26**, 12339–12350 (2006).
38. Paintlia, M.K., Paintlia, A.S., Singh, A.K. & Singh, I. Synergistic activity of interleukin-17 and tumor necrosis factor-alpha enhances oxidative stress-mediated oligodendrocyte apoptosis. *J. Neurochem.* **116**, 508–521 (2011).
39. Furuta, S. *et al.* IL-25 causes apoptosis of IL-25R–expressing breast cancer cells without toxicity to nonmalignant cells. *Sci. Transl. Med.* **3**, 78ra31 (2011).
40. Simon, C., Gotz, M. & Dimou, L. Progenitors in the adult cerebral cortex: cell cycle properties and regulation by physiological stimuli and injury. *Glia* **59**, 869–881 (2011).
41. Nishiyama, A., Chang, A. & Trapp, B.D. NG2$^+$ glial cells: a novel glial cell population in the adult brain. *J. Neuropathol. Exp. Neurol.* **58**, 1113–1124 (1999).
42. Lee, Y. *et al.* Oligodendroglia metabolically support axons and contribute to neurodegeneration. *Nature* **487**, 443–448 (2012).
43. Fünfschilling, U. *et al.* Glycolytic oligodendrocytes maintain myelin and long-term axonal integrity. *Nature* **485**, 517–521 (2012).
44. Butts, B.D., Houde, C. & Mehmet, H. Maturation-dependent sensitivity of oligodendrocyte lineage cells to apoptosis: implications for normal development and disease. *Cell Death Differ.* **15**, 1178–1186 (2008).
45. Franklin, R.J. & Ffrench-Constant, C. Remyelination in the CNS: from biology to therapy. *Nat. Rev. Neurosci.* **9**, 839–855 (2008).
46. Lev, N., Barhum, Y., Melamed, E. & Offen, D. Bax-ablation attenuates experimental autoimmune encephalomyelitis in mice. *Neurosci. Lett.* **359**, 139–142 (2004).
47. Hisahara, S., Okano, H. & Miura, M. Caspase-mediated oligodendrocyte cell death in the pathogenesis of autoimmune demyelination. *Neurosci. Res.* **46**, 387–397 (2003).
48. Mc Guire, C., Beyaert, R. & van Loo, G. Death receptor signaling in central nervous system inflammation and demyelination. *Trends Neurosci.* **34**, 619–628 (2011).
49. Hara, H., Nanri, Y., Tabata, E., Mitsutake, S. & Tabira, T. Identification of astrocyte-derived immune suppressor factor that induces apoptosis of autoreactive T cells. *J. Neuroimmunol.* **233**, 135–146 (2011).
50. Patel, J. & Balabanov, R. Molecular mechanisms of oligodendrocyte injury in multiple sclerosis and experimental autoimmune encephalomyelitis. *Int. J. Mol. Sci.* **13**, 10647–10659 (2012).

ONLINE METHODS

Mice. Act1-deficient mice on the C57BL/6J background were generated as described previously[51]. C57BL/6-Tg(GFAP-Cre)8Gtm mice were purchase from the National Cancer Institute[52]. *Cnp1-cre* transgenic mice were provided by K.-A. Nave (Max Planck Institute of Experimental Medicine). B6-Tg(Cspg4-cre)1Akik/J and B6.Cg-Tg(Eno2-cre)39Jme/J[53] mice were purchased from Jackson Laboratory. All of the mice used in this study were female unless specified otherwise. For all experiments, mice were 6–12-week-old, age-matched littermates between experimental groups. Mice were housed under specific pathogen–free conditions. Experimental protocols were approved by the Institutional Animal Care and Use Committee of Cleveland Clinic.

Induction and assessment of EAE. Active EAE was induced and assessed as previously described[16]. Passive EAE was also induced as previously described[17]. Briefly, recipient mice were injected with 3.0×10^7 polarized $MOG_{35–55}$-specific Th1 or Th17 cells 4 h after 500-Rad sublethal irradiation. To prepare $MOG_{35–55}$-specific polarized T cells, donor mice were immunized with $MOG_{35–55}$ subcutaneously; draining lymph node cells were prepared from donor mice 10 d after immunization. Cells were cultured for 5 d with $MOG_{35–55}$ at a concentration of 25 μg ml^{-1} under either Th1-polarizing conditions (20 ng ml^{-1} rmIL-12, R&D; 2 μg ml^{-1} αIL-23p19, eBioscience) or Th17-polarizing conditions (20 ng ml^{-1} rmIL-23, R&D). The clinical score was performed in double-blinded manner. For the sample size, we performed power analysis for the clinical score of EAE, which has an average of 25% coefficient of variance. We determined that with $n = 15$ mice we had 90% power to detect 30% difference between the groups.

Isolation and analysis of CNS inflammatory cells. Brains were homogenized in ice-cold tissue grinders, filtered through a 70-μm cell strainer and the cells were collected by centrifugation at 400 *g* for 5 min at 4 °C. Cells were resuspended in 10 ml of 30% Percoll (Amersham Bioscience) and centrifuged onto a 70% Percoll cushion in 15-ml tubes at 800*g* for 30 min. Cells at the 30–70% interface were collected and were subjected to flow cytometry. Fluorescence-conjugated monoclonal antibodies to CD4 (clone GK1.5), CD8 (clone 53-6.7), CD45 (clone 30-F11) and Ly6G (clone 1A8), and isotype controls were purchased from BD Biosciences. F4/80 (clone Cl:A3-1) was obtained from Serotech. The antibodies were diluted at 1:100 when used.

Histological analysis. All the sections used here were 5 μm thick. For paraffin-embedded tissue, spinal cords collected from phosphate-buffered saline–perfused mice were fixed in 10% formalin and then dehydrated with 70% alcohol. Sections were stained with either hematoxylin and eosin or luxol fast blue to evaluate inflammation and demyelination, respectively. For frozen sections, fresh spinal cords were embedded in OCT (Tissue-Tek) and snap frozen in liquid nitrogen. Sections were incubated with antibody to CD11b (BD Biosciences, M1/70, 1:200). Antigens were visualized following incubation with horseradish peroxidase–conjugated secondary antibodies (Molecular Probes). For cytohistochemical staining, cells were fixed by 2% paraformaldehyde for 10 min. Cells were further permeabilized by 0.1% Triton X-100 for 10 min, then incubated with primary antibody followed by fluorescence-conjugated secondary antibodies for microscopic analysis. NG2 antibodies were provided by W.B. Stallcup (Burnham Institute for Medical Research). Antibody to Olig2 (AB9610, 1:500) was purchased from Millipore. Antibodies to CNPase (SMI 91, 1:200) and MBP (SMI 99, 1:200) were purchased from Convance. Antibody to cleaved caspase 3 (5A1E, 1:200) was purchased from Cell Signaling Technology and antibody to GST-π (ADI-MSA-102-E, 1:1,000) was obtained from Enzo Life Science. The quantification of histology was performed in a double-blinded manner.

Primary culture of CNS resident cells. Astrocyte culture was prepared from 1-d-old neonatal mice. Briefly, brains freed of meninges were dissociated with 1-ml pipettes. Debris was removed by filtration with a 70-μm cell strainer (Falcon). Cells were cultured in DMEM plus 10% fetal bovine serum (vol/vol) supplemented with 50 μg ml^{-1} penicillin and 50 μg ml^{-1} streptomycin. After 10 d, astrocytes were stained with antibody to GFAP (Sigma, G3893, 1:500) and purity was >95%. Neurons were prepared from the pups at E15. Brains were dissociated with 1-ml pipettes and the debris removed using a 70-μm cell strainer (Falcon). Cells were cultured in Neuronbasal media (Invitrogen) plus B-27 (Invitrogen) and 50 μg ml^{-1} penicillin and 50 μg ml^{-1} streptomycin. >90% of these cultured cells expressed β-Tubulin III (a marker for neurons, antibody to β-Tubulin III was purchased from Sigma, 2G10, 1:500). The culture of OPCs was carried out as described previously[54,55]. Briefly, neurospheres were prepared at E14.5 from embryos obtained from timed pregnant females. Neurosphere medium was DMEM/F12, B27 neuronal supplement (Invitrogen), and 10 ng ml^{-1} recombinant mouse epidermal growth factor (EGF, R&D). Floating neurospheres were passaged at a 1:3 ratio in the same medium every 3–4 d. To produce pure OPCs, neurospheres were dissociated after 2–3 passages and dissociated cells were plated on poly-D-lysine–coated plates under the same medium of neurosphere, but with 10 ng ml^{-1} FGF + 10 ng ml^{-1} PDGF (Peprotech) instead of EGF. >98% of cells were Olig2$^+$ CNPase$^-$ cells after 4 d of culture, suggesting that they were OPCs. FGF and PDGF were then withdrawn to drive the maturation of OPCs for 2 d, and immunohistochemical staining suggested that >95% cells were CNPase$^+$ GFAP$^-$ β-tubulin-III$^-$, suggesting they were mature oligodendrocytes. For genotyping of *NG2-cre; Act1$^{loxP/-}$* and *NG2-cre; Act1$^{loxP/+}$* mice, OPCs from both groups were cultured as stated above for 4 d, and were collected and stained with antibody to NG2 and FITC-conjugated secondary antibodies. Following this, stained OPCs were sorted by flow cytometry. The purity of NG2$^+$ cells after sorting was >98%. Sorted cells were lysed and western blot was used to assay Act1 expression NG2$^+$ cells from *NG2-cre; Act1$^{loxP/-}$* and *NG2-cre; Act1$^{loxP/+}$* mice.

Real-time PCR. Total RNA was extracted from spinal cord with TRIzol (Invitrogen) according to the manufacturer's instructions. All gene expression results are expressed as arbitrary units relative to expression *Actb*. Fold induction of gene expression in spinal cord after EAE induction was determined by dividing the relative abundance of experimental samples by the mean relative abundance of control samples from naive mice. Primer sequences were described previously[17].

TUNEL assay. Sections from paraffin-embedded spinal cords were processed for the terminal deoxynucleotidyl transferase biotin-dUTP nick-end labeling (TUNEL) staining using a kit from the manufacturer (Roche). For apoptosis analysis of cultured cells, cells were fixed with 2% paraformaldehyde (vol/vol). The other steps for TUNEL staining followed the manufacturer's instruction. The cells were counter-stained with DAPI (4′, 6′-diamidino-2-phenylindole). Quantification was done in a double-blinded manner.

Immunoprecipitation. For co-immunoprecipitations, cell extracts were incubated with antibodies and protein A beads. After overnight incubation, beads were washed four times with lysis buffer, resolved by SDS-PAGE and analyzed by western blotting according to a standard procedure.

Statistics. Non-parametric statistics was applied to all data set. The *P* values of clinical scores were determined by two-way multiple-range ANOVA for multiple comparisons except for astrocyte-specific conditional knockout mice where a Mann-Whitney test was used for each time point (*Gfap-cre; Act1$^{loxP/+}$* versus *Gfap-cre; Act1$^{loxP/-}$*). Other *P* values were determined by Mann-Whitney test. $P < 0.05$ was considered to be significant. Unless otherwise specified, all results are shown as mean and the s.e.m.

51. Qian, Y. *et al.* Act1, a negative regulator in CD40- and BAFF-mediated B cell survival. *Immunity* **21**, 575–587 (2004).
52. Bajenaru, M.L. *et al.* Astrocyte-specific inactivation of the neurofibromatosis 1 gene (NF1) is insufficient for astrocytoma formation. *Mol. Cell. Biol.* **22**, 5100–5113 (2002).
53. Frugier, T. *et al.* Nuclear targeting defect of SMN lacking the C-terminus in a mouse model of spinal muscular atrophy. *Hum. Mol. Genet.* **9**, 849–858 (2000).
54. Pedraza, C.E., Monk, R., Lei, J., Hao, Q. & Macklin, W.B. Production, characterization and efficient transfection of highly pure oligodendrocyte precursor cultures from mouse embryonic neural progenitors. *Glia* **56**, 1339–1352 (2008).
55. Chen, Y. *et al.* Isolation and culture of rat and mouse oligodendrocyte precursor cells. *Nat. Protoc.* **2**, 1044–1051 (2007).